Mapping potentially asbestos-bearing rocks using imaging spectroscopy

G.A. Swayze[1], R.F. Kokaly[1], C.T. Higgins[2], J.P. Clinkenbeard[2], R.N. Clark[1], H.A. Lowers[1], and S.J. Sutley[1]

[1]U.S. Geological Survey, Denver, Colorado 80225, USA

[2]California Department of Conservation, California Geological Survey, Sacramento, California 95814, USA

ABSTRACT

Rock and soil that may contain naturally occurring asbestos (NOA), a known human carcinogen, were mapped in the Sierra Nevada, California, using the Airborne Visible/Infrared Imaging Spectrometer (AVIRIS) to determine if these materials could be uniquely identified with spectroscopy. Such information can be used to prepare or refine maps of areas that may contain minerals that can be asbestiform, such as serpentine and tremolite-actinolite, which were the focus of this study. Although thick vegetation can conceal underlying rock and soil, use of linear-mixture spectra calculated from spectra of dry grass and serpentine allowed detection of serpentine in some parts of the study area with up to ~80% dry-grass cover. Chaparral vegetation, which was dominantly, but not exclusively, found in areas underlain by serpentinized ultramafic rocks, was also mapped. Overall, field checking at 201 sites indicated highly accurate identification by AVIRIS of mineral (94%) and vegetation (89%) categories. Practical applications of AVIRIS to mapping areas that may contain NOA include locating roads that are surfaced with serpentine aggregate, identifying sites that may require enhanced dust control or other safety measures, and filling gaps in geologic mapping where field access is limited.

INTRODUCTION

Naturally occurring asbestos (NOA) is a potential hazard to human health because of its link to mesothelioma, lung cancer, and asbestosis (e.g., Van Oss et al., 1999). Among these minerals are chrysotile (a member of the serpentine group) and the fibrous forms of several amphiboles such as tremolite and actinolite. In California, such minerals are dominantly, but not exclusively, associated with serpentinite and ultramafic rocks, which are common in the Sierra Nevada, Coast Ranges, and Klamath Mountains (Fig. 1). Many suburban communities are expanding into areas underlain by these rocks. Pan et al. (2005) have identified an increased risk of mesothelioma among people living near sources of NOA in California. Consequently, it is desirable that these particular rock types be identified and mapped to help reduce the public's exposure to potentially NOA-bearing dust generated from them.

The U.S. Geological Survey (USGS) and the California Geological Survey conducted a joint study to test the effectiveness of "hyperspectral" imagery collected by the NASA Airborne Visible/Infrared Imaging Spectrometer (AVIRIS) in mapping exposures of potentially asbestos-bearing serpentinite and ultramafic rocks (Swayze et al., 2004). The study areas are located in Plumas and El Dorado Counties in the Sierra Nevada (Figs. 1B and 1C). These areas have abundant vegetation and are underlain by a belt of Paleozoic–Mesozoic metasedimentary and metaigneous rocks intruded by plutonic rocks. The belt contains several north- to northwest-trending fault zones, most of which, including the West Bear Mountains and Melones (Fig. 1C), include lenses of serpentinized ultramafic rocks and talc schist. To verify the effectiveness of this spectral method, AVIRIS data were collected over exposures of serpentinite and ultramafic rocks that were mapped during previous studies (e.g., Churchill et al., 2000; Churchill and Hill, 2000). Our goal was to evaluate the use of this remote sensing technology to help identify serpentine- and tremolite-actinolite-bearing rocks, which potentially contain NOA, in areas where current geologic mapping is limited.

Five AVIRIS flight lines were chosen for analysis because they covered serpentinite at progressively higher elevations, thus providing a chance to evaluate how variable plant cover affects the ability to map surface mineralogy. These lines covered portions of Flagstaff Hill, the Cosumnes River, Garden Valley, and Little Bald Mountain in El Dorado County, and Red Hill in Plumas County (Fig. 1). The Flagstaff Hill line was flown over a north-trending body of serpentinite that crops out along the exposed low-water shoreline of Folsom Lake (Fig. 2). The Garden Valley line was flown over a north-trending complex that includes serpentinite and ultramafic rocks (Fig. 3). See the GSA Data Repository[1] for data reduction, mapping methods, map validation (Tables DR1 and DR2), and

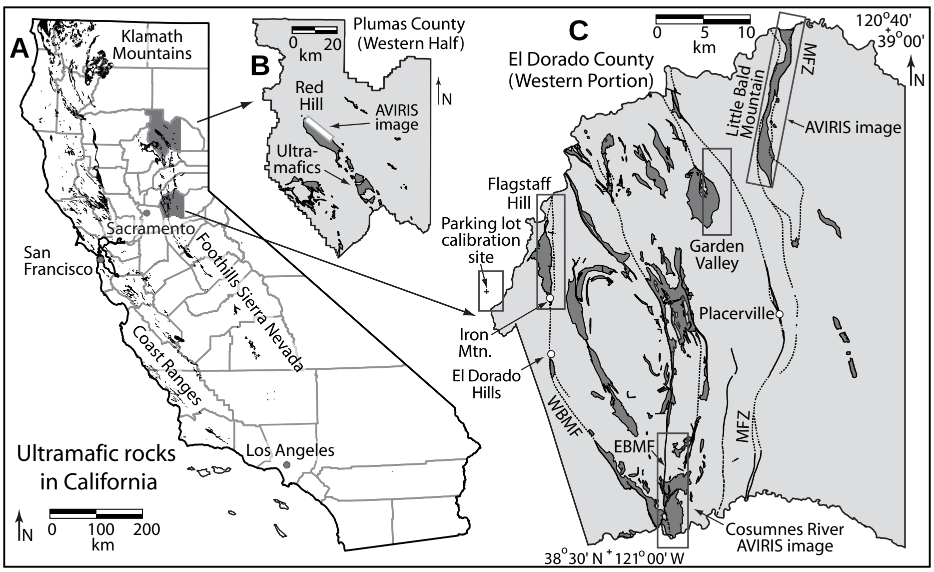

Figure 1. A: Ultramafic rocks (black) are more likely to contain naturally occurring asbestos. Modified from Churchill and Hill (2000). B: Ultramafic rocks (dark gray) exposed in western Plumas County. Rectangle shows area imaged by the Airborne Visible/Infrared Imaging Spectrometer (AVIRIS) at Red Hill. C: Areas more likely to contain asbestos (dark gray) and associated fault zones for western El Dorado County. Rectangles show areas imaged by AVIRIS. WBMF—West Bear Mountains fault; EBMF—East Bear Mountains fault; MFZ—Melones fault zone. Modified from Churchill et al. (2000).

[1]GSA Data Repository item 2009183, analytical methods and map validation, is available online at www.geosociety.org/pubs/ft2009.htm, or on request from editing@geosociety.org or Documents Secretary, GSA, P.O. Box 9140, Boulder, CO 80301, USA.

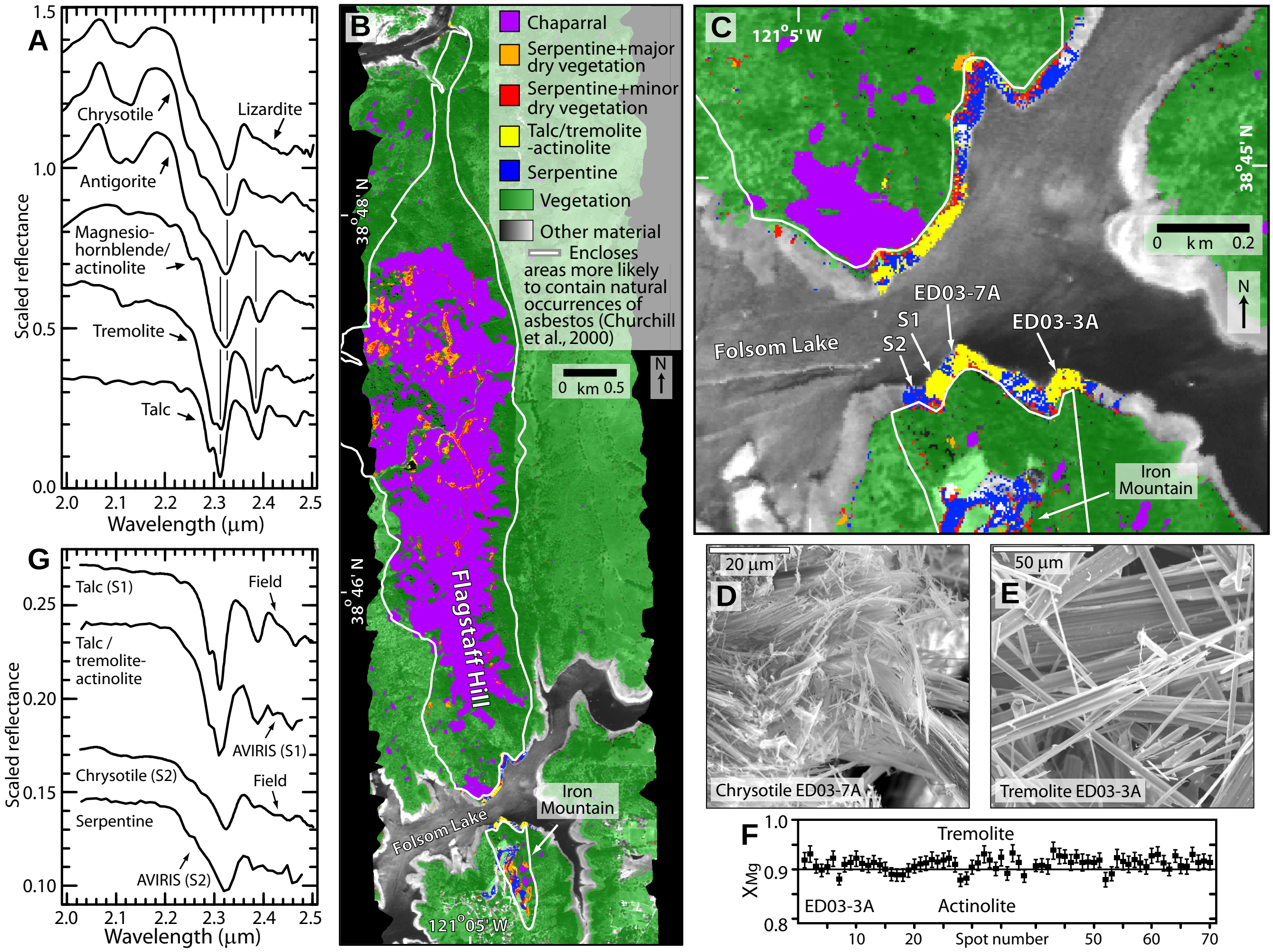

Figure 2. A: Vibrational absorptions in spectra of some reference minerals associated with serpentine deposits in El Dorado County, California. Spectra are offset for clarity; vertical lines mark positions of diagnostic tremolite and serpentine (e.g., chrysotile) absorptions. B: Map of potentially asbestos-bearing minerals, serpentine/vegetation mixtures, and chaparral vegetative cover for a portion of the Flagstaff Hill Airborne Visible/Infrared Imaging Spectrometer (AVIRIS) flight line. Vegetation category (green) refers to areas where the spectral signatures of minerals are obscured by vegetation other than chaparral. C: Details of Iron Mountain area shown in B. Sites marked ED03-7A and ED03-3A are collection locations for samples shown in D, E, and F; sites marked S1 and S2 correspond to collection locations of samples with spectra shown in G. D and E: Secondary electron images of chrysotile asbestos and fibrous to asbestiform tremolite from locations shown in C. F: Composition of fibrous tremolite from ED03-3A site measured with wavelength-dispersive electron probe microanalysis [~4% error bars; $X_{Mg} = Mg/(Mg + Fe^{2+})$]. Horizontal line at $X_{Mg} = 0.9$ separates tremolite and actinolite compositional fields. G: Lab spectra of samples from, and AVIRIS spectra of, areas S1 and S2 along the shoreline shown in C. Note that spectra of reference minerals in A and field samples in G have slightly higher spectral resolution than those measured by AVIRIS.

complete spectral maps of the study areas (Figs. DR1–DR5).

AVIRIS data were collected on 25 August 2001, around local noon. AVIRIS was flown at 5300 m altitude, producing 4 m pixels on the ground and images with swaths of ~2.5–3.0 km, depending on surface elevation. Data were calibrated to apparent reflectance and analyzed to map mineralogy and vegetation using the USGS Tetracorder system (Clark et al., 2003). Tetracorder uses a modified least-squares band-shape fitting technique to spectrally identify surface materials and create maps of their distribution. Using this technique, mineral and vegetation maps were produced from the AVIRIS data, where colored pixels represent the spatial distribution of a particular set of materials exposed on the ground surface.

MINERAL MAPPING

Although spectra of lizardite, chrysotile, and antigorite are distinct from those of nonserpentine group minerals, they have similarly shaped spectral absorptions in the 2.3 μm region (Fig. 2A). Because of their spectral similarity and because chrysotile was a minor component of the serpentinite at sites that were visited, chrysotile was grouped with the more abundant nonfibrous varieties of serpentine (i.e., lizardite and antigorite) on the maps. Because vegetation has spectral features that overlap with serpentine's 2.33 μm absorption, we used a serpentine + minor dry vegetation spectral category (red pixels with up to 30% vegetative cover) to conservatively extend mineral mapping beyond vegetation-free areas.

Tremolite has a strong absorption doublet with bands at 2.314 and 2.386 μm, which are easily distinguished from the main 2.326 μm absorption of serpentine minerals (Fig. 2A), allowing it to be detected down to 10–20 wt% in intimate mixtures with serpentine (see the GSA Data Repository for discussion). However, the spectral distinction between tremolite and Mg-rich actinolite can be subtle at AVIRIS spectral resolution, and both are spectrally similar to talc. Identification is further complicated because both amphiboles can occur with talc or in close

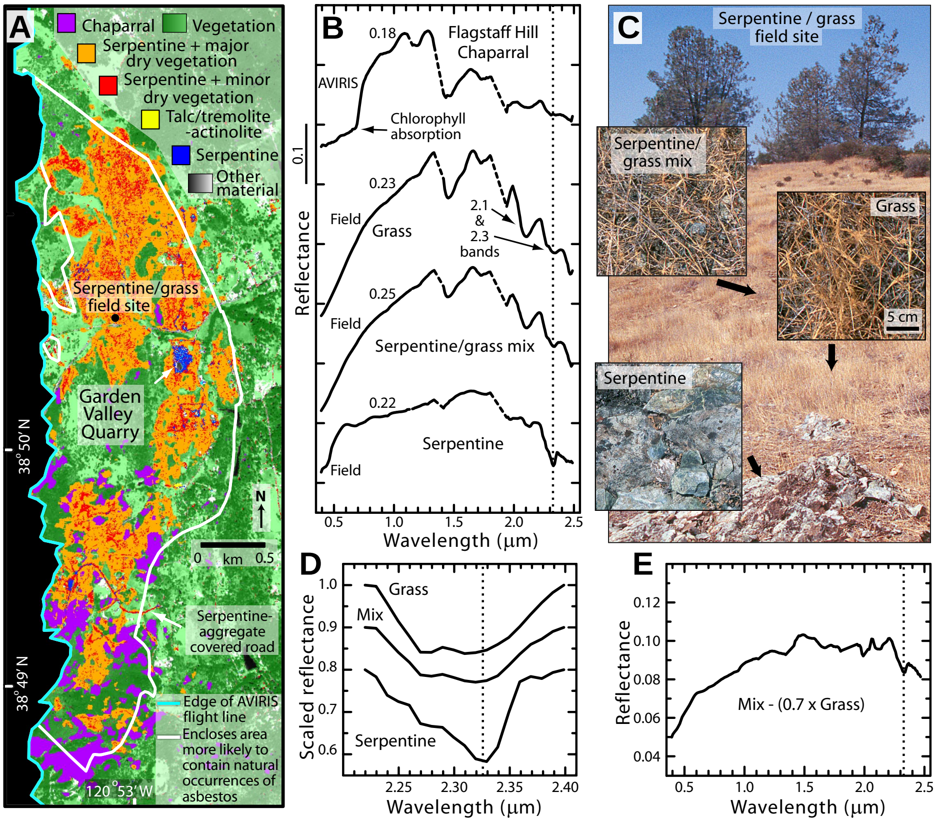

Figure 3. A: Map of potentially asbestos-bearing minerals, serpentine/vegetation mixtures, and chaparral vegetation cover for a portion of the Garden Valley Airborne Visible/Infrared Imaging Spectrometer (AVIRIS) flight line. B: Field spectra of serpentine/grass areas marked in C and an AVIRIS spectrum for an area of chaparral covered by the Flagstaff Hill AVIRIS flight line. Spectra are offset for clarity. Reflectance at 1.00 μm is given. Channels in wavelength regions of strong atmospheric absorptions were deleted from the spectra (dashed lines). The center of the serpentine absorption at 2.326 μm is plotted as a dotted line in B, D, and E. C: Photo of the serpentine/grass field site labeled in A along road right-of-way. Arrows on the photo indicate where field spectra were measured. Inset photos were taken looking straight down; all have the same scale. D: Continuum removal applied to the field spectra in B for absorption features near 2.3 μm. E: The result of subtracting the grass spectrum (multiplied by 0.70) from the mixed serpentine/grass spectrum.

proximity to it in altered ultramafic rocks. Therefore, we combined them into a single category called talc/tremolite-actinolite (T/TA) to simplify spectral mapping. A pixel was binned into the T/TA category even when these minerals were mixed with serpentine, as long as they covered more than 50% of that pixel's surface. It should be noted that not all tremolite or actinolite is fibrous, and that just because they were spectrally mapped, this does not imply they are tremolite- or actinolite-asbestos.

Figures 2B and 2C are maps of the densely vegetated Flagstaff Hill area, where most mineral exposures consist of serpentine + minor dry vegetation (red) and T/TA (yellow) along unpaved roads and in quarries. At the southern end of the hill, serpentine- and T/TA-bearing rocks are well exposed along the Folsom Lake shoreline during low-water conditions (Fig. 2C). Exposures on both shores were field checked and verified to be chrysotile-bearing serpentinite (Fig. 2D) and tremolite-talc schist. Tremolite, as determined by electron probe microanalysis, ranged from prismatic to fibrous over a distance of a few meters (Figs. 2E and 2F). Because talc is more abundant than tremolite in the schist, AVIRIS spectra from these areas match reference spectra of talc instead of tremolite-actinolite (Fig. 2G). Nonfibrous intergrown magnesiohornblende and actinolite were found in metavolcanic rocks surrounding the ultramafic body where they are exposed along the shoreline. This mineral assemblage (Fig. 2A) has a spectral signature similar to that of T/TA (Fig. 2G), but it was successfully differentiated from T/TA by Tetracorder mapping.

Areas more likely to contain NOA, as defined by Churchill et al. (2000), are shown by white-line polygons in Figures 2 and 3. These polygons enclose previously mapped ultramafic rocks, serpentinite, and their associated soils. Nearly all of the high-density clusters of pixels that mapped as serpentine, serpentine + minor dry vegetation, and T/TA fall either inside or within a few hundred meters of these boundaries except where transported by human activities. An exception is shown where the low-water condition of Folsom Lake, at the time of the AVIRIS flight, resulted in exposure of serpentine and T/TA that are outside of the polygons (Fig. 2C).

Because AVIRIS measures reflected sunlight, it cannot be used to detect minerals deeper than can typically be seen with the human eye, and hence the data can only provide information on minerals exposed in the top few millimeters of the surface when not concealed by vegetation. Consequently, areas on the images that lack colored pixels (e.g., just above the waterline) are underlain by metavolcanic rocks and soil that do not contain the minerals of interest or have too little of them for detection with AVIRIS. Laboratory spectra of simulated serpentinized ultramafic rock indicate that AVIRIS can be used to detect serpentine concentrations down to ~5–10 wt% in areas free of vegetation (see GSA Data Repository discussion). An accuracy assessment of the mineralogic categories was conducted at 93 accessible sites in the study areas. Based on these reference data, the overall accuracy of the mineral categories was 94% (Table DR1), and the Kappa coefficient (Congalton, 2001) was 0.91.

In the Garden Valley area, there are several roads outside of the ultramafic body that have the spectral signature of serpentine. Some of these roads were field checked, and each was found to be covered by crushed serpentine aggregate. Low-altitude AVIRIS maps thus appear to be effective in detecting serpentine aggregate on unpaved roads (Fig. 3A). A recent study (DTSC, 2005) found dust from serpentine road aggregate to be potentially harmful to human health. No conclusions regarding the presence or absence of asbestos in the areas identified as serpentine-bearing are possible from the AVIRIS data alone. Unequivocal identification of asbestos would require appropriate sampling and analysis of the road aggregate in those areas.

VEGETATION MAPPING

The spectral signatures of chaparral species, including *Arctostaphylus viscida*, *Adenostoma fasciculatum*, and *Heteromeles arbutifolia*, were studied to determine if they could be used to indirectly identify areas of serpentine. While not strictly confined to serpentine, these species have a local affinity for serpentine (Kruckeberg, 1984). An AVIRIS spectrum representative of chaparral was added to the Tetracorder spectral library in order to map chaparral using the shape of the 0.65 μm chlorophyll feature

(Fig. 3B). Tetracorder results were filtered with a 9 × 9 pixel majority filter to portray the dominant cover over a 36 × 36 m area. Chaparral was detected primarily, but not exclusively, in areas of ultramafic and serpentinized rock in the Flagstaff Hill and Garden Valley AVIRIS images. In the Flagstaff Hill image (Fig. 2B), 96% of the detected chaparral falls within the white-line polygons based on spatial analysis using ArcGIS®. Figure 3A shows the distribution of vegetation in a portion of the Garden Valley image. Two-thirds of the detected chaparral falls within the polygon, but some extends beyond these areas. Field inspection confirmed that chaparral, growing on gabbroic rock, extends beyond the polygon. Thus, while highly correlated with underlying serpentinized ultramafic rocks, the indication of chaparral on the spectral maps does not conclusively mean this rock type is present under every area covered by chaparral. Overall, the successful discrimination of chaparral from other vegetation using AVIRIS is consistent with previous studies (e.g., Dennison and Roberts, 2003).

To detect serpentine in areas with grass cover greater than 30%, we used the method described in Karnieli et al. (2001) for identifying multiple spectral components in a pixel, which involved adding spectra of serpentine and grass in different fractions. The serpentine and grass spectra were measured in the field with an ASD FR® spectrometer and convolved to AVIRIS spectral resolution (Figs. 3B and 3C). The 2.1 and 2.3 µm absorption features of dry grass were used for Tetracorder mapping using continuum-removed spectra in Kokaly et al. (2007).

Grass and serpentine mixtures with a grass fraction greater than 20% were detected over large portions of the Garden Valley study area; on the spectral map orange pixels indicate areas with ~30%–80% dry-grass cover on serpentinite (Fig. 3A). In both the Garden Valley and Flagstaff Hill images, 93% of these orange pixels were within the polygons. The synthetic mixtures do not include the effects of shadows cast by plant material on rock/soil substrates; therefore, detection of serpentine with 80% grass cover may be an optimistic detection limit as the contribution of serpentine material to a pixel's spectrum could be preferentially reduced by shadows.

We examined detection levels in the field by measuring spectra in an area with dense grass cover (Fig. 3C). A field spectrum of a 70% grass-covered serpentine site looks nearly identical to that of a 100% grass-covered site (Fig. 3B). However, the continuum-removed spectra (Fig. 3D) show a small shift of the absorption band center from 2.312 µm in the 100% grass spectrum to 2.319 µm in the mixed serpentine/grass spectrum, bringing it closer to the 2.326 µm serpentine absorption. As an additional check, the grass spectrum was multiplied by 0.7 (estimated fraction of grass cover at the mixture site) and then subtracted from the mixed serpentine/grass spectrum. The resulting spectrum (Fig. 3E) has a shape very similar to the serpentine spectrum in Figure 3B.

An accuracy assessment of the vegetation categories was conducted in June 2008. Field observations of grass, chaparral, and other vegetation cover and surface materials were made at 108 accessible sites in the El Dorado County study areas. The overall accuracy of the vegetation categories was 89% (Table DR2), and the Kappa coefficient (Congalton, 2001) was 0.82. A single dry-vegetation spectrum was found to be representative of dry vegetation in this study area as evidenced by the accurate results; however, more spectra may be needed to adequately represent the spectral shapes of dry vegetation in the other areas.

CONCLUSIONS

The vegetation categories are an important component of the Flagstaff Hill and Garden Valley spectral maps because chaparral and serpentine/grass mixtures covered at least half of the area within the polygons, considerably more area than is covered by mineral-related (blue and yellow) pixels on the maps. Observations from all five study areas indicate that chaparral cover is patchy to dominant on serpentinized rock at lower elevations, whereas it gives way to grass cover at intermediate elevations, with conifer forest cover dominant at the highest elevations.

Spectral maps that integrate information from substrate-dependent vegetative classification and lithologically independent mineral identification can be used as a tool for delineating areas more likely to contain NOA. These maps can also be used to identify roads surfaced with serpentine aggregate, locate areas in need of dust control, and help fill gaps in geologic mapping where access is limited. We hope that this study will motivate others to use this imaging technology to complement fieldwork when investigating areas of NOA worldwide.

ACKNOWLEDGMENTS

We thank B. Van Gosen, G. Plumlee, R. Churchill, T. King, A. Brogan, B. Martini, and four anonymous reviewers for constructive comments. We also appreciate help from the NASA Airborne Visible/Infrared Imaging Spectrometer (AVIRIS) team and the California Department of Parks and Recreation.

REFERENCES CITED

Churchill, R.K., and Hill, R.L., 2000, A general location guide for ultramafic rocks in California—Areas more likely to contain naturally occurring asbestos: California Department of Conservation, Division of Mines and Geology, Open-File Report 2000-19, 7 p.

Churchill, R.K., Higgins, C.T., and Hill, B., 2000, Areas more likely to contain natural occurrences of asbestos in western El Dorado County, California: California Department of Conservation, Division of Mines and Geology, Open-File Report 2000-002, 66 p.

Clark, R.N., Swayze, G.A., Livo, K.E., Kokaly, R.F., Sutley, S.J., Dalton, J.B., McDougal, R.R., and Gent, C.A., 2003, Imaging spectroscopy: Earth and planetary remote sensing with the USGS Tetracorder and expert systems: Journal of Geophysical Research, v. 108, no. E12, 5131, doi: 10.1029/2002JE001847.

Congalton, R.G., 2001, Accuracy assessment and validation of remotely sensed data and other spatial information: International Journal of Wildland Fire, v. 10, p. 321–328, doi: 10.1071/WF01031.

Dennison, P.E., and Roberts, D.A., 2003, The effects of vegetation phenology on endmember selection and species mapping in southern California chaparral: Remote Sensing of Environment, v. 87, p. 295–309, doi: 10.1016/j.rse.2003.07.001.

DTSC (California Department of Toxic Substances Control), 2005, Study of airborne asbestos from a serpentine road in Garden Valley, California: Sacramento, California, California Environmental Protection Agency, 48 p.

Karnieli, A., Kokaly, R.F., West, N.E., and Clark, R.N., 2001, Remote sensing of biological soil crusts, in Belnap, J., and Lange, O.L., eds., Biological soil crusts: Structure, function and managements: Berlin, Springer-Verlag, Ecological Studies, v. 150, p. 431–456.

Kokaly, R.F., Rockwell, B.W., Haire, S.L., and King, T.V.V., 2007, Characterization of post-fire surface cover, soils, and burn severity at the Cerro Grande Fire, New Mexico, using hyperspectral and multispectral remote sensing: Remote Sensing of Environment, v. 106, p. 305–325, doi: 10.1016/j.rse.2006.08.006.

Kruckeberg, A.R., 1984, California serpentines: Flora, vegetation, geology, soils, and management problems: Los Angeles, University of California Press, 180 p.

Pan, X.L., Day, H.W., Wang, W., Beckett, L.A., and Schenker, M.B., 2005, Residential proximity to naturally occurring asbestos and mesothelioma risk in California: American Journal of Respiratory and Critical Care Medicine, v. 172, p. 1019–1025.

Swayze, G.A., Higgins, C.T., Clinkenbeard, J.P., Kokaly, R.F., Clark, R.N., Meeker, G.P., and Sutley, S.J., 2004, Preliminary report on using imaging spectroscopy to map ultramafic rocks, serpentinites, and tremolite-actinolite-bearing rocks in California: U.S. Geological Survey Open-File Report 2004-1304, 20 p.

Van Oss, C.J., Naim, J.O., Costanzo, P.M., Giese, R.F., Jr., Wu, W., and Sorling, A.F., 1999, Impact of different asbestos species and other mineral particles on pulmonary pathogenesis: Clays and Clay Minerals, v. 47, no. 6, p. 697–707, doi: 10.1346/CCMN.1999.0470603.

Manuscript received 6 February 2009
Revised manuscript received 27 March 2009
Manuscript accepted 4 April 2009

Printed in USA